Eur. Phys. J. B **55**, 363–370 (2007)
DOI: 10.1140/epjb/e2007-00064-0

THE EUROPEAN PHYSICAL JOURNAL B

Monte Carlo test of the Goldstone mode singularity in 3D XY model

J. Kaupužs[1,a], R.V.N. Melnik[2], and J. Rimshans[1]

[1] Institute of Mathematics and Computer Science, University of Latvia, 29 Rainja Boulevard, 1459 Riga, Latvia
[2] Wilfrid Laurier University, Waterloo, Ontario, N2L 3C5, Canada

Received 8 August 2006 / Received in final form 17 January 2006
Published online 7 March 2007 –

Abstract. Monte Carlo simulations of magnetization and susceptibility in the 3D XY model are performed for system sizes up to $L = 384$ (significantly exceeding the largest size $L = 160$ considered in work published previously), and fields $h \geq 0.0003125$ at two different coupling constants $\beta = 0.5$, and $\beta = 0.55$ in the ordered phase. We examine the prediction of the standard theory that the longitudinal susceptibility $\chi_{\parallel}$ has a Goldstone mode singularity such that $\chi_{\parallel} \propto h^{-1/2}$ holds when $h \to 0$. Most of our results, however, support another theoretical prediction that the singularity is of a more general form $\chi_{\parallel} \propto h^{\rho-1}$, where $1/2 < \rho < 1$ is a universal exponent related to the $\sim h^{\rho}$ variation of the magnetization.

PACS. 05.10.Ln Monte Carlo methods – 75.10.Hk Classical spin models – 05.50.+q Lattice theory and statistics (Ising, Potts, etc.)

1 Introduction

It is widely believed that three-dimensional $\mathcal{O}(n)$ models with global rotational symmetry ($n \geq 2$) exhibit a Goldstone-mode singularity in the ordered phase below the critical temperature. See, for example [1–5] and references therein for the theoretical approaches further referred by us as the standard theory. These models possess a local order parameter that is represented by an n-component vector. The three-dimensional (3D) XY model simulation studied here is in this category. For such a system, the magnetization $M(h)$ is expected to behave as

$$M(h) = M(+0) + c_1 h^{1/2} \qquad \text{as} \quad h \to 0, \tag{1}$$

depending on the external field h, where $M(+0) = \lim_{h\to 0} M(h)$ is the spontaneous magnetization. Thus, the assumption here is that the longitudinal suseptibility $\chi_{\parallel}$ scales exactly as $\partial M(h)/\partial h \propto h^{-1/2}$ as $h \to 0$. However, it has been argued in [6,7] that, in principle, this cannot be the exact asymptotic behaviour (see also [8] for details of the formalism). Hence, a generalisation of equation (1) has been proposed:

$$M(h) = M(+0) + c_1 h^{\rho} \qquad \text{as} \quad h \to 0, \tag{2}$$

where $1/2 < \rho < 1$ is an exponent related to the singularity of the transverse correlation function $G_{\perp}(\mathbf{k}) \sim k^{-\lambda_{\perp}}$ in Fourier space at $h = +0$ via

$$\rho = (d/\lambda_{\perp}) - 1, \tag{3}$$

where d is the spatial dimensionality. Equation (1) is obtained from equation (2) by formally setting $\rho = 1/2$, which is consistent with the Gaussian result $\lambda_{\perp} = 2$ at $d = 3$. Some numerical support for the claims that $\rho = 1/2$, based on the observation that the Monte Carlo (MC) simulations of magnetization data, have previously been reported [9–11]. These include an additional correction term, which is consistent with the expansion in powers of $h^{1/2}$ provided by the standard theory [1–5]. The exponent ρ itself, however, has not been determined in [9–11]. Therefore, a proposal that a better fit to the data could be found using a slightly different value for ρ cannot be excluded. Some initial attempts to determine ρ for the 3D XY model from MC data have been made in [7]. However, we find here that the fields h that were used are still too large to provide reliable results. In this work the simulations are extended to much smaller fields and larger lattices, up to a linear lattice size $L = 384$. This significantly exceeds the largest size $L = 160$ simulated previously [11]. It enables us to extract the thermodynamic limit values for magnetization and susceptibility, including fields several times smaller (at a given coupling constant) than in [11]. The new data suggest that the exponent ρ has a value that is slightly larger than 1/2. In our opinion this fact has fundamental significance, since it indicates that the long-distance spin fluctuations very likely are not simply Gaussian spin waves, or noninteracting massless bosons from quantum field theory. Instead, there is a new, more complex physics behind it.

[a] e-mail: kaupuzs@latnet.lv

2 Method

Monte Carlo simulations are performed of the 3D XY model for a simple cubic lattice using the Hamiltonian $\mathcal{H}$ given by

$$\frac{\mathcal{H}}{T} = -\beta \left(\sum_{\langle ij \rangle} \mathbf{s}_i \mathbf{s}_j + \sum_i \mathbf{h}\mathbf{s}_\mathbf{i} \right), \tag{4}$$

where T is temperature, $\mathbf{s}_i$ is the spin variable (a two-component vector of unit length in the xy-plane) of the ith lattice site, β is the coupling constant, and $\mathbf{h}$ is the external field. We define that the field is oriented along the x axis. The simulations are performed in the ordered phase at $\beta = 0.5, 0.55 > \beta_c$, where $\beta_c \simeq 0.4542$ [12] is the critical point. Both the x-projection of magnetization per spin $\langle m_x \rangle$, and the longitudinal susceptibility,

$$\chi_\parallel = \frac{\partial \langle m_x \rangle}{\partial H} = V \left(\langle m_x^2 \rangle - \langle m_x \rangle^2 \right), \tag{5}$$

are evaluated for different lattice sizes L, where $V = L^3$ is the volume and $H = \beta h$.

The simulations employ both a Metropolis algorithm (for $h \geq 0.005$), and a modified Wolff's cluster algorithm (for $h \leq 0.02$). The standard Wolff's algorithm [13] is designed for zero external field $h = 0$. The external field can be introduced as an auxiliary spin which interacts with all other spins via the coupling constant $|h|\ \beta$. This spin is treated on the same grounds as others, whereas the x-projection of magnetization (given by non-auxiliary spins) is its projection on the auxiliary spin. This modification is fully analogous to that used in [9] for the Swendsen-Wang algorithm.

The Metropolis algorithm can be optimized slightly by choosing a range of allowed rotation angles $[-\varphi_{\max}, \varphi_{\max}]$ for a single spin flip that ensures about 50% probability of its acceptance. We use $\varphi_{\max} = 0.8\pi$ for $\beta = 0.5$, and $\varphi_{\max} = 0.7\pi$ for $\beta = 0.55$. In the simulations using the Metropolis algorithm for $L \leq 64$, the statistical averages are evaluated over the interval $0.08 \leq h \leq 0.32$, from $(3.2 \times 10^6) \times (64/L^2)$ sweeps, discarding at least the first 50 000 from the beginning of the simulation to ensure satisfactory equilibration. When $h < 0.08$, the total number of Monte Carlo steps in the simulation, including the discarded part, is made larger by a factor $0.08/h$. Each simulation is divided into bins, using the final 50 to estimate $\langle m_x \rangle$ and $\langle m_x^2 \rangle$, and their standard errors. The susceptibility $\chi_\parallel$ is then calculated from these values according to equation (5). The error bars are evaluated by the jackknife method [14]. When the lattice size is $L = 128$, the number of retained sweeps ranges from 60% to 100% of that for smaller lattices. When $L = 192$ this fraction is 30% to 40%. The discarded part is 50% of the whole simulation when $L = 64$, 128, and 192.

For smaller fields — where the Metropolis algorithm becomes increasingly ineffective — the simulation employs the modified Wolff's cluster algorithm. Here better results are achieved using a much smaller number of sweeps (e.g., by an order of magnitude at $h = 0.01$ and $L = 128, 192$) than the Metropolis takes. It is also not necessary to discard so much of the simulation to achieve equilibration. For the largest lattice with $L = 384$, and the smallest field $h = 0.0003125$ at $\beta = 0.5$, the calculation takes 1.35×10^5 cluster algorithm steps (collected from 3 independent runs), or about $(1.35 \times 10^5) \times$ (meanclustersize) $\simeq 2.97 \times 10^4$ sweeps. The first 1.65×10^3 sweeps are discarded from each set. A similar or somewhat larger number of sweeps are also used in other simulations that employ the modified Wolff's cluster algorithm. Although the cluster algorithm appears to be much more effective than the Metropolis one when considering small fields, a comparison between the results of both algorithms provides a useful test of validity.

Note that, in principle, significant systematic errors can occur if the random number generator is poorly implemented [15,16]. These errors, however, depend on which simulation algorithm is used. Hence, if they are present in our simulations, their effect could be seen as a discrepancy between the results obtained by the Metropolis algorithm compared with the cluster one. Since both algorithms also have completely different equilibration properties, faults here may also produce discrepancies. To avoid any possible problems caused by correlations among pseudo-random numbers, we employ a sophisticated shuffling scheme that was recently proposed and tested in [17].

3 Results

3.1 Magnetization $\langle \mathbf{m_x} \rangle$ and susceptibility $\chi_\parallel$

Calculated values of $\langle m_x \rangle$ by both algorithms at $\beta = 0.55$ for system sizes $L = 16, 32, 64, 128, 192$ over the interval $0.005 \leq h \leq 0.32$ are shown in Table 1. The extended results for smaller fields $0.000625 \leq h \leq 0.0025$ and larger lattices $L \leq 384$, obtained by the cluster algorithm, are given in Table 2.

The corresponding results for larger and smaller fields (up to $h = 0.0003125$) at $\beta = 0.5$ are presented in Tables 3 and 4, respectively.

In Tables 5–8 the results are given for susceptibility $\chi_\parallel$ using the same parameters as for the magnetization data in Tables 1–4, respectively.

In general, we observe no detectable systematic discrepancies between the results of the Metropolis and modified Wolff's algorithms. Occasionally, random deviations do occur that are slightly larger in magnitude than the estimated standard errors σ: this is expected from statistics, and is acceptable. We observe a fast convergence to the thermodynamic limit values for the simulated quantities with increasing system size. However, the smaller the field h is, the larger the size must be to reach the thermodynamic limit. It appears that the minimal acceptable size scales approximately as $\propto h^{-1/2}$. In fact, for any given h in Tables 1–8, the results for at least the two largest sizes available coincide within the simulation accuracy. Therefore, the data for largest lattice sizes provide satisfactory estimates of the thermodynamic limit values, given in Table 9.

Table 1. Calculated values of $\langle m_x \rangle$ for the 3D XY model using different lattice sizes L and external fields $h \geq 0.005$ at a fixed coupling constant $\beta = 0.55$. The underlined values are simulated by the modified Wolff's algorithm, the others are by the Metropolis algorithm.

h	$\langle m_x \rangle$				
	$L = 192$	$L = 128$	$L = 64$	$L = 32$	$L = 16$
0.005	0.639572(13)	0.639577(14)	0.639519(24)		
0.005			0.639415(74)	0.63723(16)	
0.007	0.641440(13)	0.641465(17)			
0.007	0.641481(21)	0.641440(28)	0.641372(65)	0.64035(13)	0.61905(68)
0.01	0.643955(12)	0.643975(13)	0.643955(16)		
0.01	0.643976(16)	0.643954(21)	0.643977(57)	0.64324(12)	0.62969(48)
0.014	0.646875(17)	0.646901(22)	0.646836(55)	0.646570(86)	0.63841(29)
0.02	0.650751(13)	0.650748(13)			
0.02	0.650750(16)	0.650757(16)	0.650797(46)	0.650669(67)	0.64566(20)
0.028	0.655236(13)	0.655247(15)	0.655332(42)	0.655175(73)	0.65260(14)
0.04	0.661156(12)	0.661128(12)	0.661131(42)	0.661144(58)	0.65977(13)
0.056	0.668020(12)	0.668000(14)	0.668045(39)	0.668042(51)	0.667342(85)
0.08	0.676888(12)	0.676895(13)	0.676956(42)	0.676946(55)	0.676609(87)
0.112		0.6869974(83)	0.686969(27)	0.686955(50)	0.686947(57)
0.16			0.699763(23)	0.699847(32)	0.699730(47)
0.224			0.713916(22)	0.713941(30)	0.713922(38)
0.32			0.731122(17)	0.731148(24)	0.731174(34)

Table 2. Calculated values of $\langle m_x \rangle$ by modified Wolff's algorithm for the 3D XY model using different lattice sizes L and external fields $h \leq 0.0025$ at a fixed coupling constant $\beta = 0.55$.

h	$\langle m_x \rangle$			
	$L = 384$	$L = 256$	$L = 192$	$L = 128$
0.000625	0.633431(11)	0.633426(15)		
0.00125		0.634699(11)	0.634709(14)	0.634694(18)
0.0025			0.636642(13)	0.636663(17)

Table 3. Calculated values of $\langle m_x \rangle$ for the 3D XY model using different lattice sizes L and external fields $h \geq 0.005$ at a fixed coupling constant $\beta = 0.5$. The underlined values are simulated by the modified Wolff's algorithm, the others are by the Metropolis algorithm.

h	$\langle m_x \rangle$				
	$L = 192$	$L = 128$	$L = 64$	$L = 32$	$L = 16$
0.005	0.533655(11)	0.533640(22)	0.533571(29)	0.53155(19)	
0.005			0.533567(75)	0.53123(22)	
0.007	0.536931(13)	0.536931(29)	0.536846(82)	0.53585(13)	0.51299(65)
0.01	0.541304(12)	0.541323(22)	0.541276(19)		
0.01	0.541283(23)	0.541329(23)	0.541193(59)	0.54057(12)	0.52748(36)
0.014		0.546442(24)	0.546388(68)	0.54616(11)	0.53798(28)
0.02	0.553239(14)	0.553246(16)			
0.02	0.553272(14)	0.553227(20)	0.553223(51)	0.553315(71)	0.54830(23)
0.028		0.561141(18)	0.561088(45)	0.561158(83)	0.55856(15)
0.04	0.571286(16)	0.571313(19)	0.571323(54)	0.571391(69)	0.57018(12)
0.056		0.582877(18)	0.582950(45)	0.582959(71)	0.58224(11)
0.08	0.597470(17)	0.597501(18)	0.597505(52)	0.597487(63)	0.59730(11)
0.112		0.613547(15)	0.613496(46)	0.613468(62)	0.613370(90)
0.16			0.633219(31)	0.633111(50)	0.633128(70)
0.224			0.653998(28)	0.654033(34)	0.653993(57)
0.32			0.678470(22)	0.678437(32)	0.678389(52)

Table 4. Calculated values of $\langle m_x \rangle$ by the modified Wolff's algorithm for the 3D XY model using different lattice sizes L and external fields $h \leq 0.0025$ at a fixed coupling constant $\beta = 0.5$.

h	$\langle m_x \rangle$			
	$L = 384$	$L = 256$	$L = 192$	$L = 128$
0.0003125	0.522091(13)	0.522066(23)	0.522009(28)	
0.000625		0.523453(15)	0.523436(20)	0.523253(31)
0.00125			0.525490(16)	0.525462(22)
0.0025			0.528682(15)	0.528678(22)

Table 5. Calculated values of $\chi_\parallel$ for the 3D XY model using different lattice sizes L and external fields $h \geq 0.005$ at a fixed coupling constant $\beta = 0.55$. The underlined values are simulated by the modified Wolff's algorithm, the others are by the Metropolis algorithm.

h	$\chi_\parallel$				
	$L = 192$	$L = 128$	$L = 64$	$L = 32$	$L = 16$
0.005	1.883(35)	1.825(46)	1.903(21)		
0.005			1.985(76)	3.23(12)	
0.007	1.692(43)	1.588(25)			
0.007	1.623(49)	1.635(30)	1.624(35)	2.178(69)	9.55(40)
0.01	1.419(34)	1.441(26)	1.424(11)		
0.01	1.426(35)	1.385(28)	1.455(36)	1.698(51)	5.29(25)
0.014	1.246(40)	1.258(31)	1.262(25)	1.323(20)	2.947(99)
0.02	1.105(45)	1.057(20)			
0.02	1.151(38)	1.060(19)	1.109(21)	1.121(16)	1.889(41)
0.028	0.941(29)	1.001(19)	0.925(18)	0.978(11)	1.265(19)
0.04	0.811(24)	0.811(14)	0.853(15)	0.8401(79)	0.977(13)
0.056	0.743(22)	0.718(16)	0.734(16)	0.740(10)	0.7743(71)
0.08	0.635(24)	0.642(15)	0.628(14)	0.6229(71)	0.6370(45)
0.112		0.516(13)	0.515(10)	0.5281(55)	0.5370(38)
0.16			0.4410(83)	0.4374(48)	0.4441(22)
0.224			0.3675(65)	0.3671(29)	0.3679(19)
0.32			0.2888(43)	0.2925(22)	0.2928(13)

Table 6. Calculated values of $\chi_\parallel$ by the modified Wolff's algorithm for the 3D XY model using different lattice sizes L and external fields $h \leq 0.0025$ at a fixed coupling constant $\beta = 0.55$.

h	$\chi_\parallel$			
	$L = 384$	$L = 256$	$L = 192$	$L = 128$
0.000625	4.60(13)	4.45(11)		
0.00125		3.420(80)	3.347(82)	3.346(66)
0.0025			2.373(40)	2.408(32)

A weighted average is applied over the overlaping results obtained by the two simulation algorithms, using weights that are $\propto 1/\sigma_i^2$ (with individual standard errors σ_i indicated after the tabulated values, which is the usually accepted practice for MC simulations). This minimizes the resulting statistical errors. Note that the thermodynamic limit for magnetization can be extracted in different ways, e.g., from its modulus $\langle |m| \rangle$, or from squared magnetization $\langle m^2 \rangle$ data when $L \to \infty$. We use the $\langle m_x \rangle$ data, as in [11], since the finite-size effects are smaller for the range of L and h considered in this case.

3.2 The exponent ρ

Here the exponent ρ in equation (2) is determined from the numerical data listed in Table 9. According to equation (5), equation (2) implies that

$$\chi_\parallel \propto h^{\rho - 1}. \tag{6}$$

Therefore, a singularity occurs in the longitudinal susceptibility when $h \to 0$. This provides a simple way to estimate ρ from the gradient of $\ln \chi_\parallel$ as a function of $\ln h$. This is shown in Figure 1. The linear fits yield $\rho = 0.6003(58)$ for $\beta = 0.55$, and $\rho = 0.6162(39)$ for $\beta = 0.5$. The latter result possesses a smaller value for the sum of weighted squared deviations per degree of freedom $\chi^2/N_{\mathrm{d.o.f.}}$ of the fit [18]. When $\beta = 0.55$, $\chi^2/N_{\mathrm{d.o.f.}} = 2.03$, and when $\beta = 0.5$, $\chi^2/N_{\mathrm{d.o.f.}} = 1.26$. Hence, these results support the idea that $\rho > 1/2$ holds, as proposed in [6,7]. Any such determination, however, should be taken with caution even when the fit is apparently good (as in the case

Table 7. Calculated values of $\chi_\parallel$ for the 3D XY model using different lattice sizes L and external fields $h \geq 0.005$ at a fixed coupling constant $\beta = 0.5$. The underlined values are simulated by the modified Wolff's algorithm, the others are by the Metropolis algorithm.

h	$\chi_\parallel$				
	$L = 192$	$L = 128$	$L = 64$	$L = 32$	$L = 16$
0.005	3.418(57)	3.458(56)	3.606(32)	5.07(12)	
0.005			3.564(70)	5.16(16)	
0.007	3.157(57)	3.089(69)	3.166(57)	3.640(79)	12.66(47)
0.01	2.779(46)	2.683(30)	2.743(16)		
0.01	2.743(70)	2.681(44)	2.826(43)	3.078(73)	6.98(20)
0.014		2.344(40)	2.466(47)	2.532(35)	4.368(91)
0.02	2.057(45)	2.091(26)			
0.02	2.077(70)	2.153(39)	2.116(37)	2.115(25)	3.029(63)
0.028		1.836(34)	1.830(26)	1.826(16)	2.174(24)
0.04	1.661(76)	1.618(29)	1.549(30)	1.566(17)	1.710(17)
0.056		1.324(31)	1.303(26)	1.324(15)	1.391(10)
0.08	1.186(47)	1.123(24)	1.111(26)	1.092(13)	1.1150(74)
0.112		0.941(20)	0.928(20)	0.9117(85)	0.9146(55)
0.16			0.732(14)	0.7361(72)	0.7320(33)
0.224			0.577(10)	0.5738(46)	0.5812(30)
0.32			0.4415(75)	0.4481(34)	0.4456(22)

Table 8. Caculated values of $\chi_\parallel$ by the modified Wolff's algorithm for the 3D XY model using different lattice sizes L and external fields $h \leq 0.0025$ at a fixed coupling constant $\beta = 0.5$.

h	$\chi_\parallel$			
	$L = 384$	$L = 256$	$L = 192$	$L = 128$
0.0003125	10.27(28)	10.33(33)	10.99(36)	
0.000625		7.86(15)	7.93(15)	8.87(21)
0.00125			5.83(10)	6.009(73)
0.0025			4.584(79)	4.526(59)

Table 9. The estimated thermodynamic limit values of magnetization M and longitudinal susceptibility $\chi_\parallel$ of the 3D XY model for two values of coupling constant β and different external fields h.

h	$\beta = 0.55$		$\beta = 0.5$	
	M	$\chi_\parallel$	M	$\chi_\parallel$
0.0003125			0.522091(13)	10.27(28)
0.000625	0.633431(11)	4.60(13)	0.523453(15)	7.86(15)
0.00125	0.634699(11)	3.420(80)	0.525490(16)	5.83(10)
0.0025	0.636642(13)	2.373(40)	0.528682(15)	4.584(79)
0.005	0.639572(13)	1.883(35)	0.533655(11)	3.418(57)
0.007	0.641451(11)	1.662(32)	0.536931(13)	3.157(57)
0.01	0.6439623(94)	1.422(24)	0.541300(11)	2.768(38)
0.014	0.646875(17)	1.246(40)	0.546442(24)	2.344(40)
0.02	0.6507506(99)	1.132(29)	0.5532558(99)	2.063(38)
0.028	0.655236(13)	0.941(29)	0.561141(18)	1.836(34)
0.04	0.661156(12)	0.811(24)	0.571286(16)	1.661(76)
0.056	0.668020(12)	0.743(22)	0.582877(18)	1.324(31)
0.08	0.676888(12)	0.635(24)	0.597470(17)	1.186(47)
0.112	0.6869974(83)	0.516(13)	0.613547(15)	0.941(20)
0.16	0.699763(23)	0.4410(83)	0.633219(31)	0.732(14)
0.224	0.713916(22)	0.3675(65)	0.653998(28)	0.577(10)
0.32	0.731122(17)	0.2888(43)	0.678470(22)	0.4415(75)

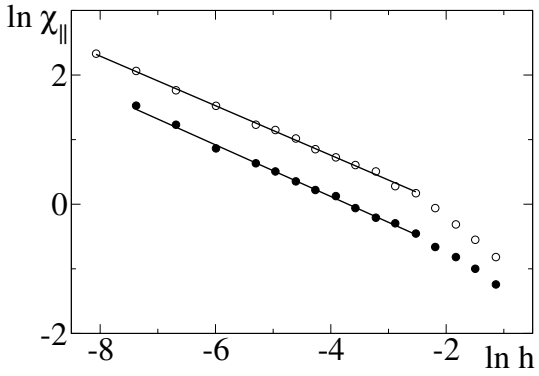

Fig. 1. Linear fits to the parallel component of $\ln \chi_{\parallel}$ plotted as a function of $\ln h$ using $\beta = 0.55$ (solid circles) and $\beta = 0.5$ (empty circles).

of $\beta = 0.5$). The gradient of the function can change very gradually, resulting in a significant discrepancy between its true value and the asymptotic one.

It is possible to make a better estimate of ρ using the more accurate magnetization data, based on the assumption that it is described by

$$M(h) = M(+0) + \sum_{n=0}^{m} c_n h^{\rho_n}, \qquad (7)$$

and making the leading exponent $\rho_0 \equiv \rho$ as the adjustable parameter, with the correction exponents $\rho_n = (n+1)/2$ being choosen according to the standard theory [4]. The results test the validity of this theory.

The number of correction terms m is varied from $m = 0$ to $m = 2$. The fitted exponent ρ is expected to converge to its true value when using smaller h, even if the fixed correction exponents are approximate. To examine the asymptotic behaviour of ρ when $h \to 0$, it is determined over several different intervals for h. These are choosen such that they should be sufficiently wide to ensure stability of the fitting procedure, while being narrow enough to have a meaningful effect on the value of $\chi^2/N_{\mathrm{d.o.f.}}$. The results for the exponent ρ at $\beta = 0.55$ and $\beta = 0.5$ are given in Tables 10 and 11, respectively. Evidently, the fits which ignore the corrections to scaling ($m = 0$), as well as those ones which include only the leading correction term ($m = 1$) place the exponent ρ closer to 0.6 than to the standard theoretical value 0.5. The values for $\beta = 0.5$ and $\beta = 0.55$, however, do not agree sufficiently well, indicating that the higher order corrections could be responsible for systematic errors in these results, leading to inconsistent values for ρ.

The fits with $m = 2$, which include also the second order correction to scaling, provide reasonably consistent and somewhat smaller values for ρ. Within the accuracy of the simulation, this confirms the theoretically expected universality of this exponent. At $\beta = 0.55$ these estimates overlap, or nearly overlap within 1σ error range with the standard value $\rho = 0.5$. However, a trend may be discerned from the data indicating that for smaller values of h, the exponent ρ is larger than 0.5. This is more noticeable when $\beta = 0.5$, where the effect appears to be statistically significant. Since theory (both the standard one and that developed in [7]) predicts that ρ is a universal quantity, it is reasonable to average over the estimates for $\beta = 0.5$ and $\beta = 0.55$ to obtain statistically more reliable values. Averages weighted using $1/\sigma_i^2$ over both sets of results for $m = 2$ at larger and smaller fields are given in Table 12. An estimate $\rho = 0.552(18)$ is obtained from the data at the smallest h values.

The average values of ρ shown in Table 12 increase for smaller fields and are significantly larger than the standard value 0.5. This supports the prediction made in [7], that the standard theory is not asymptotically exact when $h \to 0$, and that $1/2 < \rho < 1$. To be more confident about this conclusion, the influence of the finite-size effects are tested by repeating various calculations with a different data set, obtained using weighted averages over magnetization values for two largest lattices at each h, instead of only the largest lattice. Good agreement of the fit results

Table 10. The exponent ρ and $\chi^2/N_{\mathrm{d.o.f.}}$ calculated for $\beta = 0.55$ using $m = 0$, 1, or 2 correction terms in equation (7) fitted over various intervals of the field h.

m	$h \times 10^3$	ρ	$\chi^2/N_{\mathrm{d.o.f.}}$
0	2.5–14	0.6038(65)	2.10
	1.25–14	0.5969(39)	1.97
	0.625–14	0.5972(28)	1.48
	0.625–10	0.5946(36)	1.58
1	2.5–56	0.6184(99)	2.19
	2.5–40	0.597(15)	1.94
	1.25–40	0.5760(94)	2.16
	1.25–28	0.558(16)	2.25
	0.625–20	0.550(15)	1.73
	0.625–14	0.575(24)	1.70
2	2.5–112	0.531(21)	1.31
	1.25–112	0.512(13)	1.30
	0.625–80	0.514(14)	1.41
	0.625–56	0.525(21)	1.57
	0.625–40	0.537(30)	1.81

Table 11. The exponent ρ and $\chi^2/N_{\mathrm{d.o.f.}}$ calculated for $\beta = 0.5$ using $m = 0$, 1, or 2 correction terms in equation (7) fitted over various intervals of the field h.

m	$h \times 10^3$	ρ	$\chi^2/N_{\mathrm{d.o.f.}}$
0	1.25–20	0.6356(14)	2.05
	0.625–20	0.6356(10)	1.64
	0.3125–14	0.6311(15)	1.33
	0.3125–10	0.6300(18)	1.37
	0.3125–7	0.6291(29)	1.77
1	1.25–20	0.592(19)	1.04
	0.625–20	0.619(12)	1.53
	0.3125–20	0.6141(80)	1.28
	0.3125–14	0.621(13)	1.50
	0.3125–10	0.629(17)	1.82
2	0.625–40	0.525(26)	2.81
	0.625–28	0.559(37)	3.11
	0.3125–40	0.538(17)	2.41
	0.3125–28	0.561(23)	2.49

Table 12. Average values of ρ using $\beta = 0.5$ and $\beta = 0.55$, with $m = 2$ correction terms included in equation (7), fitted over various intervals of the field h. For each estimate, the first of the indicated h intervals refers to $\beta = 0.5$, while the second refers to $\beta = 0.55$.

$h \times 10^3$ intervals	ρ
0.625–40, 1.25–112	0.515(12)
0.625–28, 0.625–80	0.520(13)
0.3125–40, 0.625–56	0.533(13)
0.3125–28, 0.625–40	0.552(18)

is observed in all cases, indicating that the finite-size effects are smaller than the statistical errors. In particular, our estimate $\rho = 0.552(18)$ changes by only -0.19σ.

A disadvantage of the fits using $m = 2$ is that the results vary significantly depending on the h interval, so that it is difficult to judge on what value ρ converges. A possible reason for this could be the fact that there are too many (five) fitting parameters included. Indeed, greater numbers of fitting parameters make the results even more unstable, i.e., the variation depending on the h interval becomes larger, and the statistical errors increase. Therefore, fits with $m > 2$ probably should be avoided.

One could argue naïvely that a fit with more correction terms should be better than one with fewer. However, we need to include data for larger h to obtain statistically reliable results as m increases. Moreover, an asymptotic expansion of the form in equation (7) is expected to be well convergent and valid, only for sufficiently small fields. Therefore, using more correction terms is useless. It is not even clear whether the fits with $m = 2$ are better than those with $m = 1$. Indeed, when the largest h data are discarded, the values of ρ in Table 12 come closer to those suggested by the fits with $m = 1$. Hence, it is quite possible that the decrease in ρ which occurs when m is changed from 1 to 2, is mainly a consequence of including large fields.

Our results are consistent with the idea that the Gaussian spin wave theory provides a reasonable approximation. The standard theory reduces to Gaussian spin wave theory when $h \to 0$ in the limit of long distances or small wave vectors $\mathbf{k}$. A similar situation occurs at the critical point, where it is well-known [19] that the Fourier transform of the two-point correlation function scales as $G(\mathbf{k}) \sim k^{-2+\eta}$ (when $k \to 0$) with a small positive exponent η, instead of possessing purely Gaussian behaviour $G(\mathbf{k}) \sim k^{-2}$. Similarly, we have $G_\perp(\mathbf{k}) \sim k^{-2+\eta^*}$ for the transverse correlation function of the 3D XY model in the ordered phase at $h = +0$, where $\eta^* = 0.067(22)$ holds according to equation (3) and our current estimate $\rho = 0.552(18)$.

3.3 Spontaneous magnetization M(+0)

Table 13 shows the effect on the spontaneous magnetization $M(+0)$ of fitting the magnetization data from Table 9 to equation (7) using $m = 1$ for different, fixed

Table 13. The dependence of the spontaneous magnetization $M(+0)$ (and $\chi^2/N_{\text{d.o.f.}}$) on ρ, fitted to equation (7) using $m = 1$ over a range $H = \beta h$ for $\beta = 0.55$.

$H \times 10^4$	ρ	$M(+0)$	$\chi^2/N_{\text{d.o.f.}}$
6.875–55	0.5	0.630289(82)	2.21
	0.55	0.630580(75)	1.42
	0.6	0.630822(69)	0.81
	0.65	0.631026(63)	0.36
3.4375–55	0.5	0.630489(41)	5.06
	0.55	0.630718(38)	3.02
	0.6	0.630910(35)	1.51
	0.65	0.631071(32)	0.52

Table 14. The dependence of the spontaneous magnetization $M(+0)$ (and $\chi^2/N_{\text{d.o.f.}}$) on ρ, fitted to equation (7) using $m = 1$ over a range $H = \beta h$ for $\beta = 0.5$.

$H \times 10^4$	ρ	$M(+0)$	$\chi^2/N_{\text{d.o.f.}}$
6.25–70	0.5	0.518426(50)	3.34
	0.55	0.518969(46)	1.55
	0.6	0.519421(43)	1.05
	0.65	0.519803(40)	1.84
1.5625–25	0.5	0.519109(37)	0.90
	0.55	0.519362(34)	0.52
	0.6	0.519571(31)	0.93
	0.65	0.519747(29)	2.13

values of ρ from 0.5 to 0.65, and $\beta = 0.55$. This is repeated for $\beta = 0.5$ in Table 14. These results can be compared directly with [11]. Note that the field is now expressed as $H \times 10^4$, where $H = \beta h$. In [11], the intervals used are $10 \le (H \times 10^4) \le 50$ for $\beta = 0.55$, and $8 \le (H \times 10^4) \le 75$ for $\beta = 0.5$, where in each case $M(+0) = 0.6303(1)$ and $0.5186(1)$, respectively, and $\rho = 1/2$ [11]. In Tables 13 and 14, the closest corresponding intervals are $6.875 \le (H \times 10^4) \le 55$ for $\beta = 0.55$ and $6.25 \le (H \times 10^4) \le 70$ for $\beta = 0.5$, and both with $\rho = 1/2$, giving $M(+0) = 0.630289(82)$ and $0.518426(50)$, respectively. Thus, the agreement between the present and previous results is good; however, notice that $\chi^2/N_{\text{d.o.f.}}$ is smaller when $\rho > 0.5$, meaning that the fit to the data is better. Similar behaviour is also seen for the lower H intervals in Tables 13 and 14. Hence, these results imply that the validity of the theory cannot be tested using data for $\rho = 0.5$ only: the effect of varying the exponent on the quality of the fit must also be considered.

The above estimates of the spontaneous magnetization for $\beta = 0.55$ and $\beta = 0.5$ can also be compared with $M(+0) = 0.63071(14)$ and $M(+0) = 0.51941(11)$, respectively, derived from the results in Section 3.2, including $m = 2$ correction terms in equation (7), and ρ as the adjustable parameter.

4 Conclusions

1. Monte Carlo simulations of the magnetization and susceptibility in the 3D XY model, performed by a Metropolis algorithm and a modified Wolff's cluster

algorithm, for system sizes up to $L = 384$, and fields $h \geq 0.0003125$ (for $\beta = 0.5$) at two different coupling constants $\beta = 0.5$ and $\beta = 0.55$ in the ordered phase are reported in this work. The largest size previously reported is $L = 160$ [11]. The agreement between the simulation results by both algorithms demonstrate the validity the results (i.e., the absence of critical systematic errors), as discussed in Section 2.

2. The exponent ρ in equation (2), which characterizes the singularity of the magnetization at small fields when $h \to 0$, is evaluated in several different ways, as described in Section 3.
3. Results for magnetization data similar to [11] are given, fitted to equation (7), with $\rho = 1/2$ (Sect. 3.3). In this case the estimated values of spontaneous magnetization agree well with those given in [11]. However, we find that the data fit better with somewhat larger values of the exponent ρ. This represents an advance on the earlier work where the magnetization data are calculated without considering the effect of the exponent.

References

1. I.D. Lawrie, J. Phys. A **18**, 1141 (1985)
2. P. Hasenfratz, H. Leutwyler, Nucl. Phys. B **343**, 241 (1990)
3. U.C. Tuber, F. Schwabl, Phys. Rev. B **46**, 3337 (1992)
4. L. Schäfer, H. Horner, Z. Phys. B **29**, 251 (1978)
5. R. Anishetty, R. Basu, N.D. Hari Dass, H.S. Sharatchandra, Int. J. Mod. Phys. A **14**, 3467 (1999)
6. J. Kaupužs, Latvian J. Phys. Techn. Sciences **5**, 31 (2002)
7. J. Kaupužs, e-print `arXiv:cond-mat/0202416` v4 (2004)
8. J. Kaupužs, Ann. Phys. (Leipzig) **10**, 299 (2001)
9. I. Dimitrović, P. Hasenfratz, J. Nager, F. Niedermayer, Nucl. Phys. B **350**, 893 (1991)
10. J. Engels, T. Mendes, Nucl. Phys. B **572**, 289 (2000)
11. J. Engels, S. Holtman, T. Mendes, T. Schulze, Phys. Lett. B **492**, 492 (2000)
12. N. Schultka, E. Manousakis, Phys. Rev. B **52**, 7258 (1995)
13. U. Wolff, Phys. Rev. Lett. **62**, 361 (1989)
14. M.E.J. Newman, G.T. Barkema, *Monte Carlo Methods in Statistical Physics* (Clarendon Press, Oxford, 1999)
15. A.M. Ferrenberg, D.P. Landau, Y.J. Wong, Phys. Rev. Lett. **69**, 3382 (1992)
16. G. Ossola, A.D. Sokal, Phys. Rev. E **70**, 027701 (2004)
17. J. Kaupužs, *Proc. SPIE* **5471**, 480 (2004), see also e-print `arXiv:cond-mat/0405197`
18. W.H. Press, B.P. Flannery, S.A. Teukolsky, W.T. Vetterling, *Numerical Recipes: The Art of Scientific Computing* (Cambridge University Press, Cambridge, 1989)
19. Shang-Keng Ma, *Modern Theory of Critical Phenomena* (W.A. Benjamin, Inc., New York, 1976)